Acta Neuropathol (2006) 111: 126–138
DOI 10.1007/s00401-005-0018-8

ORIGINAL PAPER

J. A. P. van de Nes · S. Konermann · R. Nafe
D. F. Swaab

β-Protein/A4 deposits are not associated with hyperphosphorylated tau in somatostatin neurons in the hypothalamus of Alzheimer's disease patients

Received: 18 July 2005 / Revised: 27 October 2005 / Accepted: 27 October 2005 / Published online: 3 February 2006

Abstract With respect to the pathogenesis of Alzheimer's disease (AD), it has been hypothesized that amorphous plaques containing β-protein/A4 (Aβ) would locally induce cytoskeletal changes, and that neurons affected by neurofibrillary tangles (NFTs) lose their neuropeptide concentration and eventually die. To test this presumed cascade of events, the hypothalami of 14 non-demented subjects (Braak 0–III) and 28 AD patients (Braak IV–VI) aged 40–98 years were selected. The subject of our study was the nucleus tuberalis lateralis (NTL), which harbors a subpopulation of somatostatinergic neurons with extensive intrinsic interconnectivity. We used Gallyas silver staining, Congo staining, single- and double-staining with monoclonal antibody AT8 and polyclonal antibody anti-Aβ, and double-immunolabeling with AT8 and anti-somatostatin$_{1-12}$ with the following results: (1) Significant amounts of silver-staining NFTs were present in only three AD patients. (2) High densities of AT8-stained cytoskeletal changes were mainly found in aged, demented patients. (3) In contrast, large amounts of Aβ deposits were mainly observed in young and middle-aged (40–59 years) AD patients, and were very low or absent mainly in the older non-demented subjects and in AD patients. (4) Reduced anti-somatostatin staining was observed in the NTL of most AD patients, but anti-somatostatin/AT8 double-stained neurons were found virtually exclusively in aged AD patients. Thus, the occurrence of Aβ deposits and hyperphosphorylated tau formation in somatostatin cells are basically independent events, while decreased somatostatin staining only partly goes together with cytoskeletal changes in somatostatin cells in the NTL of AD patients. These observations cannot be explained by the amyloid cascade hypothesis.

Keywords Alzheimer's disease · Amyloid · Hyperphosphorylated tau · Human hypothalamus · Nucleus tuberalis lateralis · Somatostatin

J. A. P. van de Nes (✉) · S. Konermann
Institute of Neuropathology, University Hospital Essen,
Hufelandstraße 55, 45122 Essen, Germany
E-mail: johannes.van.de.nes@uni-essen.de
Tel.: +49-201-7233325
Fax: +49-201-7235927

R. Nafe
Institute of Neuroradiology, J.W. Goethe University,
Frankfurt am Main, Germany

D. F. Swaab
Netherlands Institute for Brain Research,
Amsterdam, The Netherlands

Introduction

The Alzheimer's disease (AD)-ridden brain is characterized histopathologically by large amounts of β-protein/A4 (Aβ)-containing neuropil deposits, the abundant presence of cytoskeletal changes such as neurofibrillary tangles (NFTs), neuritic senile plaques (SPs), and neuropil threads, and by a reduction in the concentration of several neuropeptides. Neuropeptide loss in AD has been found to be related to progressive cytoskeletal changes in dystrophic neurites within SPs [5, 34] and to NFT-related neuronal death, visible as "ghost" tangles [12, 60]. These observations fit the prevailing amyloid cascade hypothesis on the pathogenesis of AD very well. According to this hypothesis, Aβ fibrils in amorphous plaques locally induce progressive tau phosphorylation in affected neurons, ultimately leading to SP and NFT formation, and to neuronal death. The presumed neurotoxic effect of Aβ fibrils in relation to hyperphosphorylated tau formation in neurons has been thoroughly investigated in cell cultures [10, 14], in in vivo studies in rat brain [11, 17], and in the brains of transgenic mice [18, 33], and is the basis for the search for a therapy that will block or reduce Aβ fibril deposition, e.g., by means of voluntary exercise [1], environmental enrichment [30], or upregulation of Aβ-degrading proteases [33]. However, it is unclear whether these data from neuron cultures and experimental animal studies may be extrapolated

to the human AD brain. A recently published biochemical study revealed independent accumulations of insoluble tau and Aβ in the entorhinal cortex of aged, non-demented subjects [24].

The human hypothalamus has often been thought to be hardly affected in AD due to the presence of only some NFTs and a few SPs observed with conventional silver stains and thioflavin S in this brain structure [21, 23, 47, 49]. However, immunostaining of hyperphosphorylated tau in cell bodies and neuropil threads and anti-Aβ staining amyloid deposits appeared to clearly outnumber the low amount of classical AD changes in the hypothalamus of AD patients and also to be present to a lesser degree in that of aged, non-demented control subjects [53, 57, 59], indicating that the human hypothalamus may already be affected in a preclinical stage. The various hypothalamic nuclei appeared to react in AD in a different way to the formation of hyperphosphorylated tau, ranging from no or hardly any cytoskeletal alteration in some nuclei, such as the supraoptic and paraventricular nuclei, up to a high staining density of cytoskeletal changes at the other end of the spectrum, observed in the nucleus tuberalis lateralis (NTL) [57].

In the present paper, we study the amyloid cascade hypothesis by comparing neuropeptide stainings with the densities of cytoskeletal changes and Aβ deposits in the human NTL. This nucleus is located in the posterolateral floor of the hypothalamic tuber cinereum [55] and has been suggested to be homologous to the terete nucleus in the rat [26, 50]. The clinical consequences in relation to the occurrence of AD changes in the NTL are less well studied than in relation to those in the hypothalamic suprachiasmatic nucleus, which are accompanied by sleep–wake rhythm disruption and other circadian rhythm disturbances in AD [36, 54]. However, as strong NTL pathology in AD, Huntington's disease, and argyrophilic grain disease is accompanied by severe weight loss in these conditions in spite of normal or even increased food intake, the NTL is presumed to play a role in feeding behavior and metabolism [29]. The NTL harbors a number of anatomical and histopathological characteristics that give this nucleus some important advantages over the hippocampus and cerebral cortex for testing the validity of the amyloid cascade hypothesis with respect to changes in neuropeptide concentration. First, NTL neurons are medium-sized (25 μm), display a typical polygonal or triangular shape, have an eccentrically located nucleus, and show large and densely packed coarse lipofuscin granules in the cytoplasm. The NTL is therefore easily distinguishable from the enveloping tuberomamillary nucleus with its obviously larger-sized neurons [28, 48, 55]. Secondly, the NTL contains a major subpopulation of somatostatinergic neurons, as observed immunohistochemically [6, 41, 56] and by means of mRNA in situ hybridization [37]. The vast majority of the anti-somatostatin$_{1–12}$-stained fibers in the NTL remains within the borders of this nucleus [56, 58], indicating that somatostatin$_{1–12}$ is entirely produced by somatostatin neurons in the NTL. In contrast to other somatostatin systems in the hypothalamus and adjoining areas, the NTL is characterized immunohistochemically by intense staining with an antiserum raised against pro-somatostatin-derived splicing product somatostatin$_{1–12}$, while it does not stain with antiserum raised against somatostatin$_{15–28}$ (i.e., genuine somatostatin) in non-demented subjects [58]. The high concentration of binding sites for somatostatin in the NTL [42, 45] and the finding of baskets of somatostatin$_{1–12}$-immunoreactive axonal terminals around NTL neurons [56] point to an extensive neuronal connectivity of somatostatin neurons within this nucleus. Taken together, these observations suggest that the vast majority of somatostatin cells in the NTL represent interneurons that maintain an extensive connectivity within this nucleus. This idea is further supported by the observations that massive neuronal loss in the NTL of Huntington's disease patients [27] is accompanied by a consistent decrease in somatostatin staining in this nucleus, while somatostatin immunoreactivity in the enveloping tuberomamillary nucleus stained with equal intensity in Huntington's disease patients and non-demented controls [56]. Thirdly, the NTL is mainly affected by early stages of cytoskeletal changes and Aβ deposits in AD. While the NTL of AD patients may show high amounts of "pretangle" cytoskeletal changes, as observed also in the cerebral cortex of AD patients, as shown by antibodies like Alz-50 [28, 48, 57, 59] or AT8 [52], argyrophilic NFTs are only rarely found in the NTL of AD patients [25, 40, 43]. In addition, the NTL also shows virtually exclusively Aβ deposits of the Congonegative type, i.e., amorphous plaques, but the relative proportion of amorphous plaques and "pretangle" cytoskeletal changes seems to vary with age in this nucleus. Large amounts of Aβ deposits had been found earlier in two younger AD patients, aged 40 and 45, while many Alz-50-stained cytoskeletal changes had been found in older patients, aged 56, 70, and 90 years [59].

The aim of the present study was to determine the relative density of cytoskeletal changes characterized by hyperphosphorylated tau, silver-stained NFTs, Aβ deposits, and immunohistochemical staining of somatostatin-related peptides in the NTL of 42 subjects with increasing degrees of cortical neurofibrillary degeneration, as characterized by the stages Braak 0–VI, in order to validate the proposed amyloid cascade hypothesis with respect to the somatostatinergic cell population in this nucleus.

Materials and methods

Subjects, tissues, and stainings

Human brain material was obtained by means of the rapid autopsy system of the Netherlands Brain Bank (NBB; coordinator: Dr. R. Ravid), which supplies postmortem specimens from clinically well-documented and neuropathologically confirmed cases. Permission

for brain autopsy and use of the brain and clinical data for research purposes was obtained by the NBB. Subject of study was the hypothalamic NTL of 42 patients aged 40–98. The cases were selected on the basis of the degree of cortical neurofibrillary pathology according to Braak and Braak's staging procedure (Braak 0–VI) [7] and, as AD-related cytoskeletal pathology may co-exist with argyrophilic grain disease-related cytoskeletal alterations in the NTL [9], also on the complete absence of argyrophilic grain disease-related cytoskeletal changes in the tuberal region of the human hypothalamus, including the NTL, ventromedial hypothalamic nucleus, and fornix [51]. The 14 patients staged Braak 0–III were non-demented and did not suffer from any neurological or psychiatric disorder; the 28 patients scored Braak IV–VI suffered from AD. The selected cases were also scored A, B, or C according to Braak and Braak's grading system of cortical amyloid accumulation [7]. For clinicopathological information on the subjects studied, see Table 1. Formalin-fixed, paraffin-embedded hypothalami were serially cut coronally into 6-μm-thin sections. Each 50th section was stained with thionine (0.1% thionine in acetate, pH 4) for general orientation. Sections of each subject were (1) stained with the silver iodide stain according to Gallyas [15] to recognize argyrophilic NFTs, (2) stained with the Congo stain to visualize β-amyloid cores, (3) single-stained with the AD-related altered tau antibody AT8, (4) with amyloid β-peptide antiserum (anti-Aβ), (5) double-labeled with anti-Aβ and AT8, and (6) double-stained using anti-somatostatin$_{1-12}$ (S320) and AT8.

The IgG mouse monoclonal antibody AT8 (Innogenetics, Ghent, Belgium), developed by Mercken et al. [38], detects both early pretangle and late tangle cytoskeleton alterations [8] by recognizing hyperphosphorylated sites at serine 202 and threonine 205 of the

Table 1 Clinicopathological information

		ND	AM	Age (years)	Sex (m/f)	pmd (h)	fdur (days)	pH	ApoE	Cause of death
1.	81/267	0	0	43	m	22.35	53	n.a.	n.a.	Non-Hodgkin lymphoma
2.	94/324	0	0	49	m	22.20	33	6.59	33	Sepsis
3.	82/161	0	0	57	f	45.25	35	n.a.	n.a.	Mitral stenosis
4.	79/4724	0	n.a.	59	m	2.30	53	n.a.	n.a.	Emphysema, pneumothorax
5.	79/4725	0	A	72	f	20.15	53	n.a.	n.a.	Endocarditis lenta
6.	82/175	0	B	85	m	6.15	44	n.a.	n.a.	Bronchopneumonia
7.	98/032	I	C	82	f	0.45	35	6.33	43	Multi-organ failure
8.	94/157	I	C	85	f	5.10	28	6.95	33	Pneumonia
9.	93/020	I	C	92	m	2.30	33	6.93	n.a.	Myocardial infarction
10.	98/200	II	0	74	f	7.25	31	6.95	32	Necrosis of the intestines
11.	95/160	II	0	80	m	4.30	24	6.12	33	Renal insufficiency
12.	98/091	II	0	87	m	7.25	34	6.80	33	Cardiac arrest
13.	97/073	III	C	87	m	4.00	33	7.39	33	Myocardial infarction
14.	96/297	III	A	90	f	6.10	25	6.54	33	Cardiac arrest
15.	97/349	IV	C	79	m	5.45	47	6.41	43	Pneumonia
16.	94/329	IV	C	85	m	6.15	29	6.30	33	Pyelonephritis, renal failure
17.	99/029	IV	C	86	f	3.45	32	7.08	43	Myocardial infarction
18.	93/286	IV	C	91	m	6.00	31	6.51	n.a.	Unknown
19.	89/166	V	C	40	m	2.50	28	6.46	32	Cachexia
20.	89/345	V	C	51	m	23.00	102	n.a.	n.a.	Bronchopneumonia
21.	91/92	V	C	54	f	3.15	28	6.32	33	Cachexia
22.	85/050	V	C	56	f	21.30	48	n.a.	n.a.	Pneumonia
23.	98/242	V	B	75	m	5.15	34	6.39	43	Respiratory insufficiency
24.	97/220	V	B	78	f	3.10	33	6.72	43	Cachexia
25.	94/078	V	C	83	f	4.55	36	6.18	43	Unknown
26.	95/162	V	C	84	f	4.40	27	6.28	43	Cachexia and dehydration
27.	86/364	VI	C	45	m	4.00	119	n.a.	n.a.	Cachexia
28.	90/262	VI	C	49	m	4.25	33	6.17	43	Epilepsy
29.	95/340	VI	C	57	m	5.00	45	7.00	43	Urosepsis, pneumonia
30.	96/051	VI	C	58	m	5.10	27	6.99	33	Cachexia
31.	97/109	VI	C	59	f	3.55	29	6.48	43	Sudden deterioration
32.	92/362	VI	C	63	f	4.55	38	6.50	33	Unknown
33.	94/028	VI	C	64	m	3.40	30	6.26	43	Unknown
34.	88/252	VI	C	66	m	3.15	25	6.50	33	Cachexia and sepsis
35.	83/170	VI	C	70	f	3.30	34	n.a.	n.a.	Epileptic insults
36.	91/071	VI	C	73	m	4.30	30	6.49	43	Respiratory insufficiency
37.	98/252	VI	C	78	f	5.00	39	6.73	43	Cachexia and dehydration
38.	93/057	VI	C	87	f	3.00	32	6.50	43	Viral pneumonia
39.	94/282	VI	C	87	f	5.00	33	6.66	43	Cachexia
40.	86/004	VI	C	90	f	2.30	34	n.a.	n.a.	Dehydration
41.	86/001	VI	C	97	m	5.00	40	n.a.	n.a.	Dehydration
42.	91/084	VI	C	98	f	3.30	31	6.54	43	Decompensatio cordis

ND stage of cortical neurofibrillary degeneration adapted from Braak and Braak (1991), *AM* stage of cortical amyloid pathology adapted from Braak and Braak (1991), *sex(m/f)* sex (male/female), *pmd(h)* postmortem delay (in hours), *fdur* fixation duration, *n.a.* not available

AD-modified tau molecule [18]. AT8 was slightly more sensitive to hyperphosphorylated tau than AD-related altered tau antibody Alz-50 [8]. In addition, AT8 did not show staining in control hypothalami [52], indicating that this antibody does not react with components of normal somatostatin neurons, unlike Alz-50 [58]. AT8 also appeared to be particularly useful in double-immunofluorescence experiments used to study the susceptibility of somatostatin neurons to develop AD-related cytoskeletal changes [60]. Rabbit anti-amyloid β-peptide (anti-Aβ; Zytomed, Berlin, Germany) raised against a 30 amino acid peptide derived from full-length (1–43 amino acid) amyloid β-peptide was used to visualize Aβ deposits. Rabbit antiserum S320 (#10.01.83), raised against somatostatin$_{1-28}$ (or pro-somatostatin)-derived peptide fragment somatostatin$_{1-12}$ [3, 4], was chosen, as staining with this antiserum was intensive in the NTL of non-demented subjects, while staining with anti-somatostatin$_{15-28}$ (i.e., genuine somatostatin) did not reveal any immunoreaction in this nucleus [58]. In radioimmunoassays, cross-reactivity of anti-somatostatin$_{1-12}$ with peptide fragment somatostatin$_{15-28}$ was absent and minimal with somatostatin$_{1-28}$ ($<0.01\%$). The antigenic determinant of somatostatin$_{1-12}$ appeared to be located on its carboxy(C)-terminal amino acid sequence 5–12 [4, 39]. Staining with anti-somatostatin S320 disappeared following preabsorption with neuropeptide somatostatin$_{1-12}$ [4, 39, 56]. No cross-reactivity was found following adsorption with other peptides [6]. In this paper, somatostatin staining refers to somatostatin$_{1-12}$ staining, unless stated otherwise.

AT8 immunostaining

Following deparaffination, hydration, and a standard protocol designed to prevent non-specific binding [57], two sections per patient were incubated with AT8 (1:2000) at room temperature (RT) for 1 h and then overnight at 4°C. The next day, secondary antibody incubation was performed using the indirect streptavidine-biotin-alkalic phosphatase method with biotinylated anti-broad spectrum immunoglobulins (AP125 Zytochemplus, Zytomed). Visualization of the reaction product was obtained with Fast Red as chromogen, which led to a red precipitate at a minimal background staining. The sections were counterstained with 0.1% haemalune. Omission of the primary or secondary antibody in the AT8 staining sequence resulted in complete absence of staining.

Amyloid β-peptide immunostaining

Two sections per patient were deparaffinized, hydrated, and pretreated with 98–100% formic acid (Merck, Munich, Germany) for 30 min in order to improve Aβ immunoreactivity [25] followed by the standard protocol. The sections were incubated with anti-Aβ (1:100) for 1 h at RT, followed by overnight incubation. Secondary antibody incubations and coloring of the reaction product were carried out as described above. The sections were counterstained with 0.1% haemalune. Omission of the primary or secondary antibody in the anti-Aβ staining sequence resulted in absence of staining.

Double-immunostaining with anti-Aβ and AT8

One section was used for double-immunolabeling using AT8 and anti-Aβ according to Van de Nes et al. [59]. Briefly, following deparaffination, hydration, and 98–100% formic acid (Merck) pretreatment for 30 min and 4–5 times rinsing in tap water, rabbit polyclonal anti-Aβ was used in the first sequence. Mouse monoclonal AT8 (1:1,000) was used in the second sequence. Aβ staining was obtained with 0.05% 3,3′-diaminobenzidine tetrahydrochloride (DAB), while AT8 staining was achieved with DAB enhanced with 0.25% nickel ammonium sulfate. In between the staining sequences, methanol hydrogen peroxide series were performed, according to Axelson and Van Leeuwen [2], to inhibit the remaining horseradish peroxidase activity of the first staining sequence. Following this step, the yellow-brown Aβ plaque staining did not shift to purple-black staining, proving that no HRP activity was left.

Double-immunostaining with anti-somatostatin$_{1-12}$ (S320) and AT8

Four sections per patient were used for the double-immunofluorescence experiments with anti-somatostatin$_{1-12}$ (S320) and AT8. Deparaffination and hydration were followed by antigen retrieval. Since antigen retrieval appeared to be essential for optimal staining in both neurites and perikarya in the NTL with anti-somatostatin$_{1-12}$ [56], the sections were transferred into a jar containing citrate buffer solution (0.1 M, pH 6), put into a water bath, and heated at 90°C for 30 min. Following the standard protocol, the sections were incubated simultaneously with AT8 (1:2,000) and anti-somatostatin S320 (1:1,000) at RT for 1 h, and then overnight at 4°C. The next day, the sections were incubated in carbocyanide-2 conjugated with anti-mouse IgG (Cy2, 1:100, Dianova, New York, NY, USA) and carbocyanide-3 conjugated with anti-rabbit IgG (Cy3, 1:100, Dianova) in the dark at RT for 6 h. An additional step was the incubation of the immunostained sections in a 0.3% solution of Sudan Black B (Merck) in 70% alcohol at RT for 10 min to prevent autoimmunofluorescence caused by the lipofuscin granules in NTL neurons. If not blocked, autoimmunofluorescence made any analysis of a specific immunofluorescence signal impossible [46]. The sections were then dehydrated, mounted in Eukitt, and stored in the dark until examination. S320/AT8 double-stained sections were examined with a NIKON Eclipse 600

conventional microscope equipped with the tools necessary for immunofluorescence. The fluorochromes Cy2 and Cy3 were excited with light at 465–495 and 540/25 nm, respectively. A dichroic beam splitter (505 and 565 nm, respectively) and emission bandpass filters (515–555 nm for Cy2 and 605/55 nm for Cy3) were used to generate images.

Method specificity of S320/AT8 double-immunofluorescence was checked as follows: (1) immunofluorescence with S320 displayed fine, granular cell bodies and thin, beaded fibers, while filamentous structures in perikarya and neuropil threads were recognized by AT8; (2) omission of the primary or secondary antibody in the S320 staining sequence resulted in absence of staining. The same held true when the primary or secondary antibody in the AT8 staining sequence was omitted; (3) no significant staining differences were observed between adjacent single- and double-labeled sections.

The human hypothalamus harbors a number of somatostatin-containing cell populations and projection systems [6, 40, 41]. The ventromedial hypothalamic nucleus and the NTL are located at the similar coronal level in the tuberal region of the hypothalamus (Fig. 1). The fiber bundle in the ventromedial hypothalamic nucleus functions as an internal positive control for staining with anti-somatostatin$_{1–12}$ in the NTL. Staining of the beaded fiber bundle in the ventromedial hypothalamic nucleus of AD patients by anti-somatostatin$_{1–12}$ S320 did not differ significantly from that in control subjects [40].

Estimation of the stainings and statistical methods

The NTL in each hypothalamic section was evaluated blind to the type of patient and to the presence of argyrophilic profiles, AT8-stained cell bodies and neuropil threads, anti-Aβ immunoreactive neuropil deposits, and the anti-somatostatin staining intensity in fibers and cell bodies. The stainings did not differ significantly

Fig. 1 Somatostatin$_{1–12}$ staining in the tuberal region of the human hypothalamus. Note the intensive somatostatin staining in the nucleus tuberalis lateralis and its clear delineation from its surroundings. *n* nucleus tuberalis lateralis, *v* ventromedial hypothalamic nucleus, *t* tuberomamillary nucleus, *i* infundibular nucleus, *b* bed nucleus of the stria terminalis, *f* fornix, *o* optic tract

per patient throughout the nucleus and were estimated in a semi-quantitative way. The presence or absence of silver-stained tangles was scored as follows: – = none or hardly any, 1 = some, and 2 = a significant number. AT8 and Aβ staining densities were graded to the following scale: – = none or negligible, 1 = a small amount, 2 = a moderate amount, and 3 = a large amount, while the somatostatin staining density was rated according to the following degrees: 3 = intensive, 2 = a minor reduction, 1 = a clear reduction, and – = virtually absent. The presence or absence of somatostatin/AT8 double-stained cells in the NTL was estimated as follows: – = none or hardly any, 1 = some, 2 = a considerable number. The relative densities of the AT8, anti-Aβ, and somatostatin stainings and the relative number of somatostatin/AT8 positive cells in the NTL per patient were used for statistical analysis.

Statistical analysis was performed with the SPSS software (SPSS, Chicago, USA). Regression analysis was carried out in order to test the influence of the patient's age on the immunohistochemical stainings for AT8, anti-Aβ, anti-somatostatin, and the co-expression of somatostatin and hyperphosphorylated tau. In addition, the χ^2-test was performed to test for a significant association between the Braak 0–IV and V–VI stages and each of these four stainings, and for a significant association between the immunoreactions with AT8, anti-Aβ, and anti-somatostatin. Differences were considered statistically significant at the $P < 0.05$ level.

Results

Gallyas silver-iodide staining

Argyrophilic NFTs, including "ghost" tangles, were rare in the NTL of the subjects studied. Moderate numbers of NFTs were only observed in the NTL of three aged subjects out of the 16 most seriously affected patients (Braak VI; #35, #37, and #42).

AT8 immunohistochemical staining

The NTL was affected by AT8-stained cytoskeletal changes from Braak stage III onwards. A significant association was found between Braak stages 0–IV vs V–VI and AT8 staining (χ^2-test, $P < 0.001$), showing that a more pronounced AT8-staining was present in higher Braak stages. An age-related staining pattern was present in Braak V–VI patients. The relative density of AT8-stained cell bodies and neuropil threads in the NTL of the five younger AD patients (40–54 years of age) appeared to be low or virtually absent, while AT8 staining was intensive in the NTL of all demented patients aged 70 years and older (Fig. 2a). Regression analysis showed a positive association between the density of AT8-stained cytoskeletal changes and the patient's age ($r = +4.027$, $P = 0.050$). The borderline significance is mainly due to the highly variable AT8 staining densities in the NTL of the demented middle-aged patients aged 56–66 years (Table 2 and Fig. 3).

Congo staining and amyloid β-peptide immunoreactivity

Hardly any congophilic cores were observed in the NTL in non-demented subjects and AD patients (data not shown), indicating that virtually all Aβ-reactive deposits in the NTL were amorphous plaques. The amounts of amorphous plaques in the NTL varied, but Aβ staining showed a significant negative association with the patient's age (regression analysis: $r = -9.266$, $P = 0.001$), due to the preferential presence of amorphous plaques in presenile cases (< 65 years). Four younger AD patients (aged 40, 45, 51, and 54 years; #19–21 and #27) showed considerable amounts of Aβ deposits, while the demented patients aged 56–64 years mostly displayed lower densities of Aβ deposits. Anti-Aβ staining in the NTL of the majority of the older subjects (staged Braak III–VI) was low or negligible (Fig. 2b), with the exception of considerable amounts of Aβ deposits in the NTL of one AD patient aged 78 years (#37). The lack of Aβ staining observed in the NTL of most aged AD patients contrasts with the extensive staining of amyloid deposits in the cerebral cortex, staged B or C, of all AD patients. Strong Aβ staining in the NTL was significantly associated with AD, since it was only observed in Braak V–VI patients (χ^2-test: $P = 0.001$).

Comparison of AT8 and anti-Aβ staining after double-labeling

Confirming the single-immunohistochemical stainings, large amounts of amorphous plaques were mainly observed in young AD patients (40–59 years at age) and the presence of many AT8-stained cytoskeletal changes was mainly found in the older group of AD patients aged 70 years and more (Fig. 2c, d).

Neither formalin fixation duration up till 53 days (#1, #4, and #5), nor postmortem delay up till 45 h (#3), nor the agonal state assessed by pH measurement of the cerebrospinal fluid, which ranged from 6.12 (#11) to 7.39 (#13), affected the staining with anti-somatostatin$_{1-12}$ (S320). The beaded fiber bundle entering the ventromedial hypothalamic nucleus stained intensively positive (not shown), thus functioning as internal positive control for staining in the NTL of 40 out of the 42 cases studied. Only the two AD cases with considerably larger formalin fixation times, i.e., 102 days (#20) and 119 days (#27), showed a weakly stained fiber bundle in the ventromedial hypothalamic nucleus. The very weak and negative stainings in the NTL of these patients were therefore not taken into consideration.

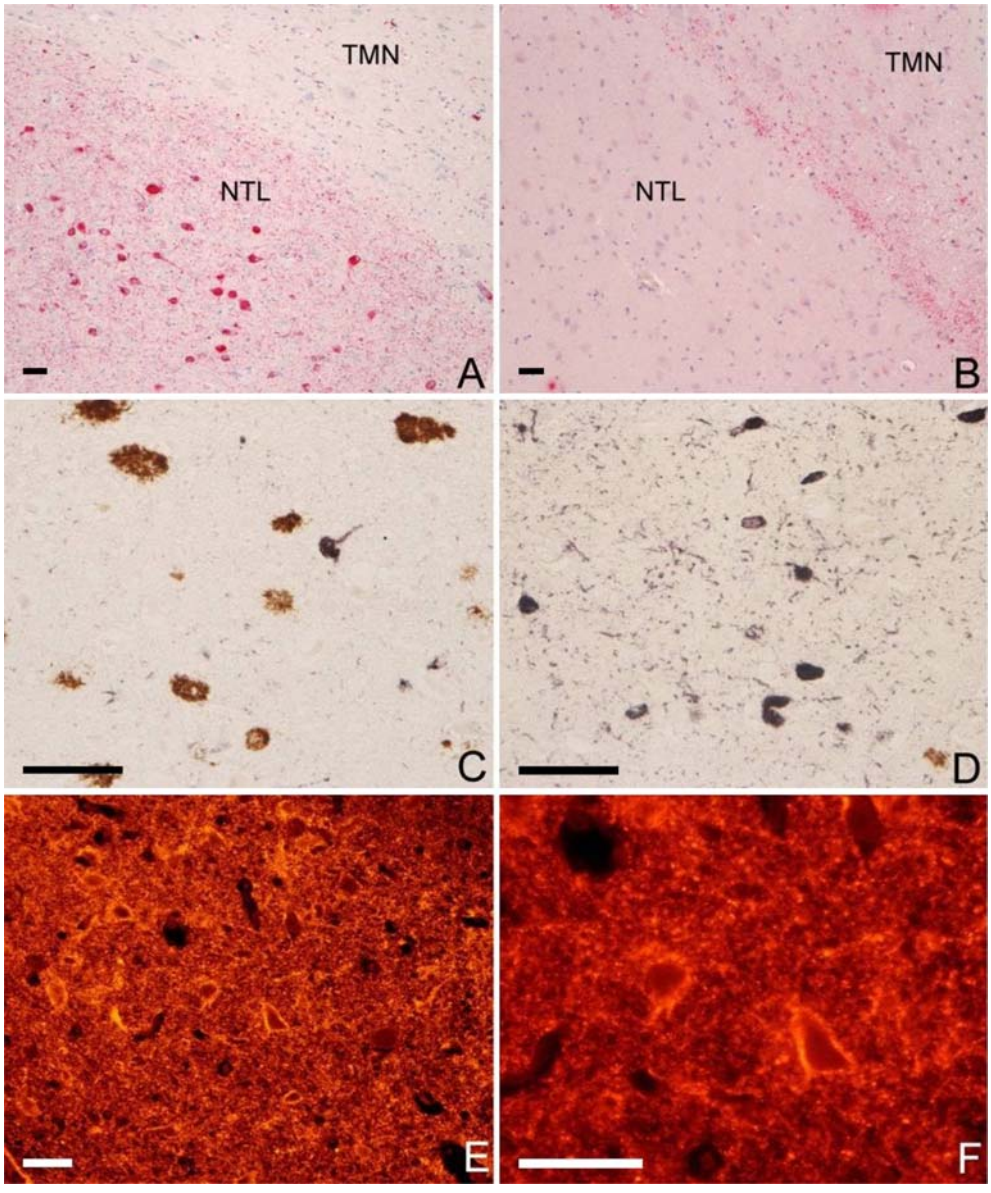

Fig. 2 a The nucleus tuberalis lateralis (*NTL*) is heavily stained with AT8. It can easily be delineated from the enveloping tuberomamillary nucleus (*TMN*), in which the density of cytoskeletal changes is low (#37). **b** The NTL is also easily distinguishable from the tuberomamillary nucleus (*TMN*) using anti-Aβ. The NTL shows hardly any Aβ deposits, while their density in the tuberomamillary nucleus is obviously higher (#30). **c** The NTL of a 51-year-old demented patient (#20) shows considerable amounts of Aβ deposits stained brown, while that of AT8-stained cell bodies and neuropil threads stained black is low. In contrast, **d** the NTL of a 90-year-old demented patient (#40) shows large amounts of AT8-stained cytoskeletal changes stained black, while the number of Aβ deposits stained brown is virtually absent. **e** The NTL of non-demented subjects shows an intensive neuronal network of very thin, beaded fibers containing somatostatin$_{1-12}$-like peptides stained orange-red as observed in this 92-year-old subject (#9). **f** Magnification of figure **e** Somatostatinergic cells reveal a patchy, granular staining in cell bodies and neurites. The scale bars represent 100 μm

Somatostatin staining in Braak 0–IV patients

All non-demented subjects (staged Braak 0–III, #1–14) displayed an intensive diffuse NTL staining of numerous thin, beaded fibers and a moderate amount of patchy, granular perikarya (Fig.. 2e, f). Two out of the four Braak IV subjects showed the same intense somatostatin staining (#15–16), while the other two AD-demented Braak IV patients displayed a reduced somatostatin staining (#17–18).

Comparison of somatostatin staining with AT8 and anti-Aβ in Braak V–VI patients

NTL neurons expressing somatostatin may contain hyperphosphorylated tau in Braak V–VI patients (Fig. 4a–d). There was a significant association between the presence of somatostatin/AT8 double-staining cells and AT8 staining density (χ^2-test: $P = 0.001$), as somatostatin/AT8 double-stained neurons were found in particular in AD patients with many cytoskeletal changes in the NTL. However, there was no significant association between somatostatin/AT8 double-stained cells and Aβ staining (χ^2-test: $P > 0.124$).

Intensive somatostatin staining in patchy, granular cell bodies and thin, beaded fibers was observed in five AD patients (Fig. 4a, b), while reduced somatostatin staining was found in 17 demented patients. Diminished somatostatin staining meant mainly loss of thin, beaded fiber density. A clearly reduced number of anti-somatostatin$_{1-12}$ immunoreactive neurons were generally found when the fiber density was low. A significant association was found between AT8 and somatostatin staining (χ^2-test, $P < 0.001$), as most cases with a decrease in somatostatin staining were associated with

Table 2 Gallyas silver staining and AT8, Aβ, and anti-somatostatin (SOM) immunoreactivity in the nucleus tuberalis lateralis in patients staged Braak 0–VI

	ND	AM	Gallyas	AT8	Aβ	SOM	SOM/AT8
1.	0	0	–	–	–	3	–
2.	0	0	–	–	–	3	–
3.	0	0	–	–	–	3	–
4.	0	n.a.	–	–	–	3	–
5.	0	A	–	–	–	3	–
6.	0	B	–	–	–	3	–
7.	I	C	–	–	–	3	–
8.	I	C	–	–	–	3	–
9.	I	C	–	–	–	3	–
10.	II	0	–	–	–	3	–
11.	II	0	–	–	–	3	–
12.	II	0	–	–	–	3	–
13.	III	C	–	1	1	3	–
14.	III	A	1	1	–	3	–
15.	IV	C	–	2	1	3	–
16.	IV	C	–	1	1	3	–
17.	IV	C	–	2	–	2	–
18.	IV	C	–	1	–	2	–
19.	V	C	–	1	3	3	1
20.	V	C	–	–	2	1*	–
21.	V	C	–	1	2	3	–
22.	V	C	–	3	1	1	–
23.	V	B	–	3	1	1	1
24.	V	B	1	3	–	1	2
25.	V	C	1	3	1	2	1
26.	V	C	–	2	1	2	2
27.	VI	C	–	1	3	–*	–
28.	VI	C	–	–	1	1	–
29.	VI	C	–	–	1	3	–
30.	VI	C	–	1	1	1	–
31.	VI	C	–	2	2	3	1
32.	VI	C	1	2	1	2	–
33.	VI	C	–	1	1	3	–
34.	VI	C	–	2	–	2	1
35.	VI	C	2	3	1	1	1
36.	VI	C	1	3	–	1	2
37.	VI	C	2	3	2	2	2
38.	VI	C	1	3	–	1	2
39.	VI	C	1	3	1	1	1
40.	VI	C	–	3	–	1	–
41.	VI	C	–	2	–	2	–
42.	VI	C	2	3	1	1	2

ND stage of cortical neurofibrillary degeneration adapted from Braak and Braak (1991), *AM* stage of cortical amyloid pathology adapted from Braak and Braak (1991), *n.a.* not available

Gallyas silver staining: – none or hardly any neurofibrillary tangles, *1* some neurofibrillary tangles, *2* a significant number of neurofibrillary tangles

AT8 immunoreactivity: – none or negligible, *1* a small amount of cytoskeletal changes, *2* a considerable amount of cytoskeletal changes, *3* a large amount of cytoskeletal changes

Anti-Aβ immunoreactivity: – none or negligible *1* a small amount of Aβ deposits *2* a considerable amount of Aβ deposits, *3* a large amount of Aβ deposits

SOM (somatostatin$_{1–12}$-like) immunoreactivity: *3* intensive beaded fiber density and cell body staining, *2* a minor reduction in beaded fiber density and intensive cell body staining, *1* a clear reduction in beaded fiber density and minor reduced cell body staining, – virtually absent staining, * not to be taken into consideration due to a formalin fixation duration >100 days

SOM/AT8 double-immunostaining: – no or hardly any somatostatin cells containing hyperphosphorylated tau, *1* some somatostatin cells containing hyperphosphorylated tau, *2* a considerable number of somatostatin cells containing hyperphosphorylated tau

the presence of higher densities of AT8-stained cell bodies and neuropil threads in the NTL (Fig. 4c, d) and vice versa (cf Table 3). However, while the fiber bundle in the ventromedial hypothalamic nucleus as internal positive control stained intensively, a clear reduction in somatostatin staining, together with low or negligible amounts of AT8-stained structures, was observed in the NTL of two young AD patients aged 49 and 58 years at death (#28, #30; Fig. 4e, f). No significant association with the patients' age was found for somatostatin staining (regression analysis: $P=0.361$).

There was a significant association between Aβ and reduced somatostatin staining (χ^2-test: $P=0.003$), as both histopathological changes were found in the NTL of most AD patients. However, there was no correlation between Aβ and somatostatin-staining densities according to the likelihood quotient ($P=0.313$). Note that in the NTL of the 49- and 58-year-old demented patients (#28 and #30), low amounts of Aβ deposits were accompanied by reduced somatostatin staining, while high amounts of anti-Aβ immunoreactive neuropil deposits went together with an unchanged dense somatostatin staining in the NTL of three AD patients aged 40, 54, and 59 years (#19, #21, and #31, respectively).

Discussion

The currently prevailing concept on the pathogenesis of AD is the amyloid cascade hypothesis. According to this hypothesis, neurotoxic Aβ fibrils in amorphous plaques locally induce progressive tau hyperphosphorylation in affected neurons, and reduced neuropeptide transmitter concentration is considered to be the final consequence of NFT-associated neuronal death. In the present paper, this cascade of events was validated by comparing the concentration of somatostatin and related peptide fragments with the densities of cytoskeletal changes and Aβ deposits in the nucleus tuberalis lateralis, as indicated by the Braak and Braak's stages of the progression of cortical neurofibrillary degeneration. The NTL was chosen for this study, because it displayed an intrinsic somatostatin subpopulation with extensive anti-somatostatin$_{1–12}$ staining in neurites and perikarya in non-demented subjects [56, 58], and because it seemed to be disproportionately affected by Aβ deposits and cytoskeletal changes in aged, non-demented, and AD patients [59]. The major finding of the present paper is that the amyloid cascade hypothesis does not seem to hold for the somatostatin cell population in the NTL of AD patients.

The hypothesis that NFT formation is followed by reduced neuropeptide expression was supported by the observation that significant amounts of argyrophilic profiles in the NTL seemed, at first glance, to be accompanied by diminished somatostatin staining. However, this relationship was found only in 3 out of the 12 most severely affected AD patients (Braak VI; #35, #37, and #42). Reduction of somatostatin staining

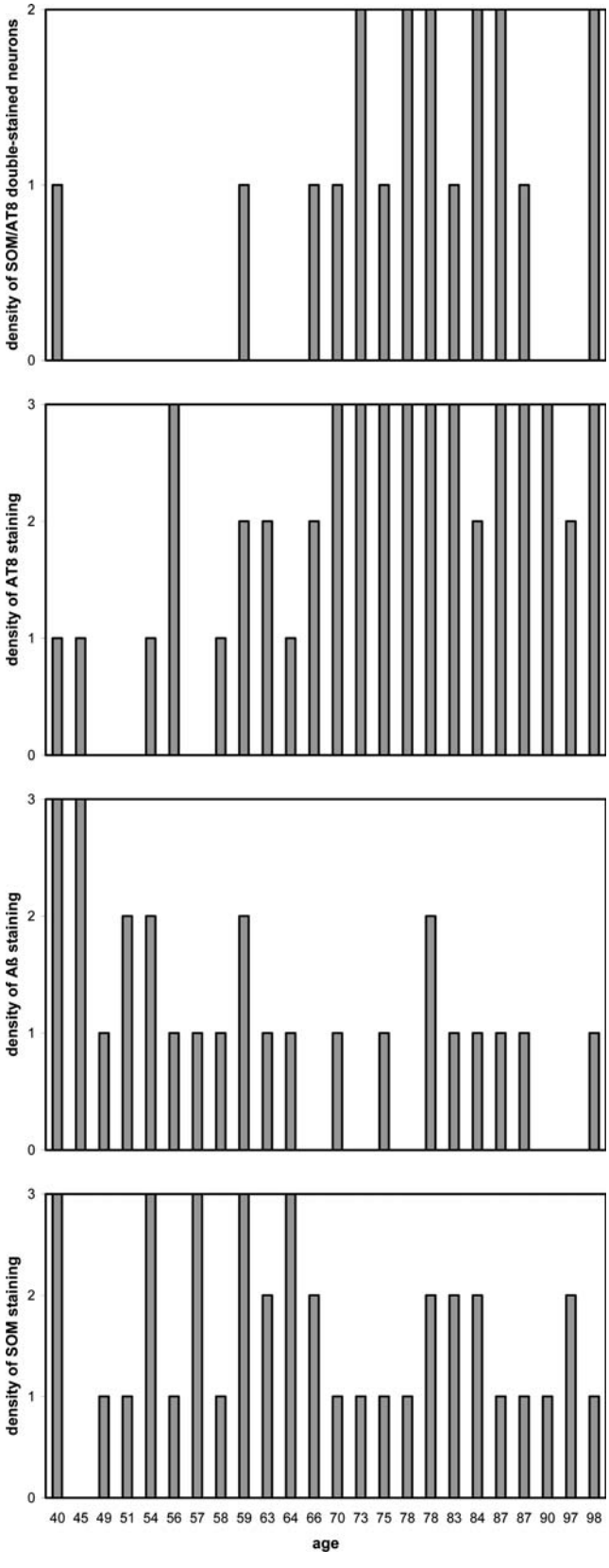

Fig. 3 Relative densities of SOM/AT8 double-stained neurons, AT8, Aβ, and somatostatin (*SOM*) stainings in Alzheimer patients staged Braak V–VI. Anti-somatostatin/AT8 double-stained neurons are mainly seen in the NTL of aged demented patients, which stain heavily for AT8 immunoreactive cytoskeletal changes. Large amounts of amorphous plaques are mainly found in young AD patients. Reduction in somatostatin staining is observed in most AD patients, irrespective of age. Thus, the occurrence of hyperphosphorylated tau in somatostatin cells does not seem to be induced by Aβ deposits, and reduced somatostatin staining cannot be due solely to the dense cytoskeleton changes. For criteria of the immunohistochemical scores, see Table 2

rather seemed to occur in the NTL of AD patients, heavily stained with non-argyrophilic, AT8-stained (''pretangle'') cytoskeletal changes. The lack of correlation between hyperphosphorylated tau formation in somatostatin neurons and amorphous plaque deposition did not support the hypothesis that the occurrence of AD-related cytoskeletal changes would be locally induced by Aβ-containing deposits. Hardly any somatostatin/AT8 double-stained neurons were observed in the NTL of young Braak V–VI patients, in spite of a significant presence of amorphous plaque density in this nucleus at a younger age. In addition, hyperphosphorylated tau formation in somatostatin cells in the NTL appeared to occur mainly in aged demented patients, while amorphous plaque density in the NTL of these patients was mainly very low, and, in some of these patients, even absent.

The NTL stains with antibodies raised against somatostatin$_{1–12}$ and does not stain with anti-somatostatin$_{15–28}$ [58]. This does not mean that anti-somatostatin$_{1–12}$ staining of cell bodies and thin, beaded fibers in the NTL represents non-specific immunoreactivity, as method-, antiserum-, and antigen-specificity have been examined carefully [3, 4, 6, 54, 56]. Staining with anti-somatostatin$_{1–28}$ S309, able to recognize the N-terminal amino acid sequence 1–11 of the pro-somatostatin molecule in radioimmunoassays [3, 4], also gives an intensive staining in the NTL of non-demented subjects [56]. In addition, staining with anti-somatostatin$_{1–12}$ and anti-somatostatin$_{1–28}$ and no staining with anti-somatostatin$_{15–28}$ as observed in the NTL has also been repeatedly noted in the neocortex of non-demented subjects [12, 20]. Apparently, the somatostatin cell population in the NTL is stained by antisera which recognize the N-terminal part of somatostatin$_{1–28,}$ and not by antisera raised against its C-terminal part. One can only speculate why. One possibility is that somatostatin neurons in the NTL differ in premortem metabolic processing and/or postmortem degradation from those neurons and projections in the hypothalamus which are positive for all three types of somatostatin antisera, such as the densely beaded fiber projection in the ventromedial hypothalamic nucleus and somatostatin cells in the tuberomamillary nucleus [56]. Another possibility is that somatostatin$_{15–28}$-like compounds are more critically affected by the histological procedures than are somatostatin$_{1–12}$-like compounds [13].

The 14 non-demented subjects and 28 AD patients studied were selected on the basis of the staging procedure according to Braak and Braak [7], viz., on the basis

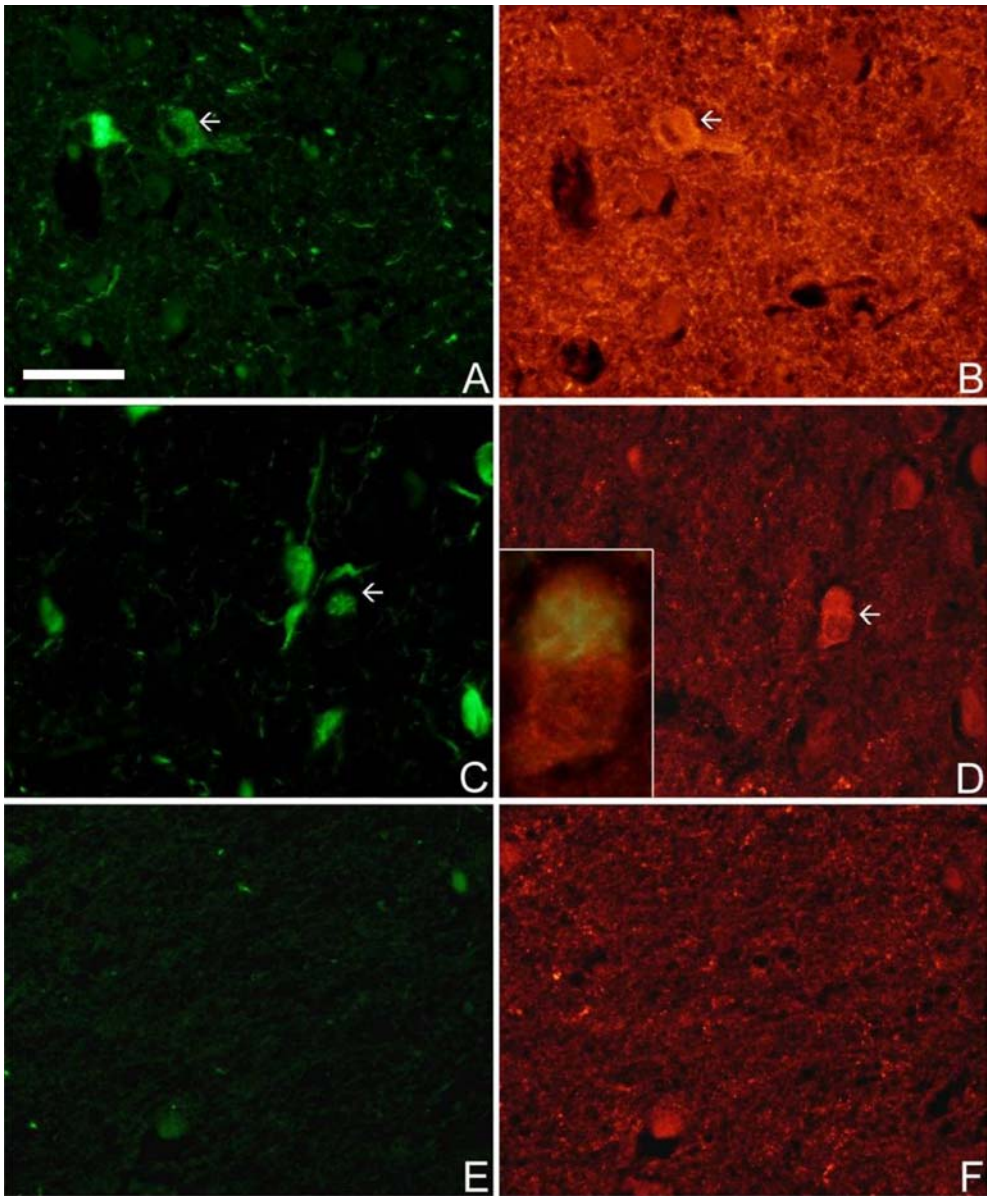

Fig. 4 a, b The NTL of the 59-year-old Braak VI patient (#31) reveals considerable amounts of AT8-immunoreactive cytoskeletal alterations stained green (**a**), while the beaded fiber density as stained orange-red with anti-somatostatin$_{1-12}$ appears as intensive (**b**) as observed in that of the 92-year-old, non-demented subject depicted in Fig. 2 **e**, **f**. Thus, somatostatin staining may remain unchanged in the NTL of AD patients. One neuron appears double-labeled with AT8 and anti-somatostatin (*arrows*). **c, d** The NTL in an aged AD patient (98-year-old Braak VI patient #42) shows large amounts of AT8-immunoreactive cell bodies and neuropil threads stained green, which are accompanied by clear reduction of somatostatin-containing fibers stained orange-red (**d**). Some neurons stain for both hyperphosphorylated tau and somatostatin. One of these neurons (see *arrows* in **c** and **d**) showing AT8/somatostatin double-labeling is depicted at a higher magnification in the *left* corner in **d. e, f** Hardly any AT8-stained cytoskeletal changes stained green and a very low anti-somatostatin staining fiber density stained orange-red were observed in the NTL of 2 young AD patients, here that of the 58-year-old Braak VI patient (#30). Thus, clear reduction in somatostatin staining in the NTL of AD patients is not necessarily accompanied by the accumulation of hyperphosphorylated tau in this nucleus. The *scale bar*, which represents 100 μm, applies to all figures

of the distribution of argyrophilic neurofibrillary changes in the hippocampal area, limbic system, and neocortex. Higher Braak stages were accompanied by gradual increase in the density of AT8-stained cytoskeletal changes in the NTL in aged controls and AD patients. However, in the NTL of the younger AD patients, AT8 staining intensity appeared to be quite variable. Some presenile AD patients showed similar high densities of AT8-stained cytoskeletal changes as observed in senile AD patients. Other young AD patients displayed clearly lower amounts of AT8-immunoreactive cell bodies and neuropil threads in the NTL. These observations indicate that AD pathology in the NTL does not necessarily correlate with Braak and

Table 3 Somatostatin staining in relation to AT8 staining

	–	1	2	3	*n*
AT8 = –	0	1	0	13	14
AT8 = 1	0	1	1	6	8
AT8 = 2	0	0	5	2	7
AT8 = 3	0	9	2	0	11
					n-total = 40

Note that in most cases an increase in AT8 staining density tends to be accompanied by reduced somatostatin staining and vice versa, leading to a significant relationship between both stainings (χ^2-test: $P < 0.001$). However, the presence of no or few cytoskeletal changes and low somatostatin staining in the NTL of two patients point to an alternative, non-hyperphosphorylated tau-related effect on the somatostatin staining. For criteria of the immunohistochemical scores, see Table 2

Braak's stages of cortical neurofibrillary degeneration, and suggest that a given age threshold is needed to make the NTL neurons more susceptible to hyperphosphorylated tau formation.

A previous study on the distribution and relative densities of amyloid deposition and cytoskeleton changes in the hypothalamus of five AD patients and five age-matched control subjects revealed the presence of large amounts of amorphous plaques in the NTL of the two young AD patients (aged 40 and 45 years) and many cytoskeletal changes in the three older demented subjects (aged 56, 70, and 90 years). In addition, the NTL in the 90-year-old non-demented control contained the same low amounts of amorphous plaques as that in the three older AD patients. Amorphous plaques and cytoskeletal changes in the NTL thus seemed to be inversely related and to show a cross-over in the course of aging [57]. This pattern has now been confirmed by the Aβ and AT8 staining densities observed in the NTL of an extended group of 28 AD patients (aged 40–98 years). Amorphous plaques were indeed mainly observed in younger AD patients (< 65 years) and showed a significant negative association with the patient's age, while there was a positive association between AT8 staining density and the age of the demented patient studied. The present study also shows, for the first time, that in the older group of ten non-demented persons and 13 AD patients (> 65 years), AT8 staining density of cytoskeletal alterations in the NTL tended to increase from Braak stage III onwards, while amorphous plaque density mainly remained very low in this nucleus. The lack of Aβ staining in the NTL of aged AD patients is not related to an overall scarcity of cortical amyloid pathology, as the cerebral cortex of all AD patients studied displayed an extensive staining of amyloid deposits. These observations suggest that the age-associated susceptibility of NTL neurons to develop cytoskeletal changes cannot be explained by Aβ fibril deposition within this nucleus.

Data from transgenic mice studies with mutants for β-amyloid precursor protein and tau protein in the same mouse suggest that Aβ deposition might trigger or facilitate the accumulation of tau [35, 43]. However, these observations do not seem to hold for the human NTL, in which Aβ accumulation and hyperphosphorylated tau formation appear as inversely related AD phenomena with a cross-over during aging. In addition, Aβ accumulation alone is insufficient to trigger the development of cytoskeletal changes [16, 22]. The introduction of transgenes expressing mutant β-amyloid precursor protein and mutant tau protein in the same mouse is required to visualize the concomitant manifestation of amyloid plaques and NFTs [35], and only a triple-transgenic mouse model with mutants for β-amyloid precursor protein, tau, and presenilin showed both amyloid plaques and tau pathology with a temporal and region-specific AD-like distribution pattern [43, 44]. The observations from mutant mice models with two or three transgenes, each forming the basis for one histopathological AD change, rather seem to support our observations in the human NTL that amyloid deposition, hyperphosphorylated tau formation, and loss of neuronal function occur basically independent of each other.

Our observations in the NTL suggest that the amyloid cascade hypothesis should be reconsidered. Some alternative pathogenetic mechanisms can be proposed. First, Aβ accumulation may be neuroprotective instead of neurotoxic [31]. Such a mechanism could explain why the gradual decrease in Aβ plaque density in the NTL from the sixth decade onwards is accompanied by an increased susceptibility of NTL neurons to develop cytoskeletal changes as a sign of neurodegeneration. An alternative possibility states that hyperphosphorylated tau formation in neurites and cell bodies occurs as a compensatory response mounted by neurons against oxidative stress [32]. However, this concept could only explain the observation that a high staining density of cytoskeletal alterations in the NTL is mainly present in the group of AD patients aged 70 years and older. A third possible mechanism is suggested by the observation that AT8-stained cell bodies and neuropil threads were present from Braak stage III onwards, but somatostatin/AT8 double-labeled neurons were only found in the NTL of aged Braak V and VI patients. Why NTL neurons expressing somatostatin show a low susceptibility for developing AD-related cytoskeletal changes should be further investigated.

In summary, while high amorphous plaque densities tended to occur mainly in the NTL of young AD patients, cytoskeletal changes in its somatostatin cells mainly occurred in the aged AD patients. Large amounts of amorphous plaques were not accompanied by diminished somatostatin staining, as observed in the NTL of three presenile AD patients (#19, #21, and #31). Reduced somatostatin staining tended to be related to an increased density of AT8-stained cytoskeletal changes and vice versa, but was also found in the NTL of two young AD patients aged 49 and 58 years (#28 and #30), with only very few AT8-stained cell bodies and neuropil threads in this nucleus. Thus, reduction in somatostatin concentration did not consistently occur in the NTL of AD patients, but, when present, seemed to be just as

much related to NFT formation and dense "pretangle" cytoskeletal changes as to a non-hyperphosphorylated tau-related type of neuronal alteration. In conclusion, Aβ deposition, hyperphosphorylated tau formation, and reduced somatostatin concentration in the NTL occur basically independently, rather than by a linear pathogenetic sequence, as proposed by the amyloid cascade hypothesis.

Acknowledgements Brain material was obtained from the Netherlands Brain Bank in the Netherlands Institute for Brain Research, Amsterdam, The Netherlands (Coordinator: Dr. R. Ravid). The neuropathological diagnoses were performed by Dr. W. Kamphorst, Institute of Pathology of the Free University Hospital in Amsterdam, The Netherlands. Anti-somatostatin$_{1-12}$ (S320) was generously provided by Dr. R. Benoit, Montreal, Canada. Mr. B. Fisser (Netherlands Institute for Brain Research, Amsterdam, The Netherlands) and Ms. S. Richter (Institute of Neuropathology, University Hospital Essen, Germany) are thanked for their technical assistance. NIKON, Düsseldorf, Germany (Mr. M. Stremmel) is greatly acknowledged for the assistance in taking the images. Ms. W. Verweij (Netherlands Institute for Brain Research, Amsterdam, The Netherlands) is thanked for editing help.

References

1. Adlard PA, Perreau VM, Pop V, Cotman CW (2005) Voluntary exercise decreases amyloid load in a transgenic mice model of Alzheimer's disease. J Neurosci 25:5217–4221
2. Axelson JF, Van Leeuwen FW (1990) Differential localization of estrogen receptors in various vasopressing synthesizing nuclei of the rat brain. J Neuroendocrinol 2:209–216
3. Benoit R, Ling N, Alford B, Guillemin R (1982) Seven peptides derived form pro-somatostatin in the rat brain. Biochem Biophys Res Commun 107:944–950
4. Benoit R, Bohlen P, Ling N, Esch F, Baird A, Ying SY, Wehrenburg WB, Guillemin R, Morrison JH, Bakhit C, Koda L, Bloom F (1984) Somatostatin-28($_{1-12}$)-like peptides. In: Patel YC, Tannenbaum GS (eds) Somatostatin. Plenum Press, New York, NY, pp 89–107
5. Benzing WC, Brady DR, Mufson EJ, Armstrong DM (1993) Evidence that transmitter-containing dystrophic neurites precede those containing paired helical filaments within senile plaques in the entorhinal cortex of nondemented elderly and Alzheimer's disease patients. Brain Res 619:55–68
6. Bouras C, Magistretti PJ, Morrison JH, Constantidinis J (1987) An immunohistochemical study of pro-somatostatin-derived peptides in the human brain. Neuroscience 22:781–800
7. Braak H, Braak E (1991) Neuropathologic stageing of Alzheimer-related changes. Acta Neuropathol 82:239–259
8. Braak E, Braak H, Mandelkow E-M (1994) A sequence of cytoskeleton changes related to the formation of neurofibrillary tangles and neuropil threads. Acta Neuropathol 87:554–567
9. Braak H, Braak E (1998) Argyrophilic grain disease: frequency of occurrence in different categories and neuropathological diagnositic criteria. J Neural Transm 105:801–819
10. Busciglio J, Lorenzo A, Yeh J, Yankner BA (1995) β-amyloid fibrils induce tau phosphorylation and loss of microtubule binding. Neuron 14:879–888
11. Chambers CB, Sigurdsson EM, Hejna MJ, Lorens SA, Lee JM, Muma NA (2000) Amyloid-β injection in rat amygdala alters tau protein but not mRNA expression. Exp Neurol 162:158–170
12. Chan-Palay V (1986) Somatostatin immunoreactive neurons in the hippocampus and cortex shown by immunogold/silver intensification on vibratome sections: coexistence with neuropeptide Y neurons, and effects of Alzheimer disease. J Comp Neurol 260:201–223
13. Coulter HD, Elde RP (1978) Somatostatin(SOM) radioimmunoassay and immunofluorescence in the rat hypothalamus: effects of dehydration with alcohol and fixation with aldehydes and OsO_4.) Anat Rec 190:369–370 (abstract)
14. Ferreira A, Lu Q, Orecchio L, Kosik KS (1997) Selective phosphorylation of adult tau isoforms in mature hippocampal neurons exposed to fibrillar Aβ. Mol Cell Neurosci 9:93–96
15. Gallyas F (1971) Silver staining of Alzheimer's neurofibrillary changes by means of physical development. Acta Morphol Acad Sci Hung 19:1–8
16. Games D, Adams D, Allessandrini R, Barbour R, Berthelette P, Blackwell C, Carr T, Clemens J, Donaldson T, Gillespie F, Guido T, Hagopian S, Johnson-Wood K, Khan K, Lee M, Leibowitz P, Lieberburg I, Little S, Masliah E, McConiugue I, Mantoya-Zavaia M, Mucke L, Paganini L, Penniman E, Power M, Schenk D, Seubert P, Snyder B, Soriano F, Tan H, Vitale J, Wadsworth S, Wolozin B, Zhao J (1995) Alzheimer-type neuropathology in transgenic mice overexpressing V717F β-amyloid precursor protein. Nature 373:523–527
17. Geula C, Wu CK, Saroff D, Lorenzo A, Yuan M, Yankner BA (1998) Aging renders the brain vulnerable to amyloid β-protein neurotoxicity. Nat Med 4:827–831
18. Goedert M, Jakes R, Vanmechelen E (1995) Monoclonal antibody AT8 recognises tau protein phosphorylation at both serine 202 and threonine 205. Neurosci Lett 189:167–170
19. Gotz J, Chen F, van Dorpe J, Nitsch RM (2001) Formation of neurofibrillary tangles in P301L tau transgenic mice induced by Aβ42 fibrils. Science 293:1491–1495
20. Hayes TL, Cameron JL, Fernstrom JD, Lewis DA (1990) A comparative analysis of the distribution of pro-somatostatin-derived peptides in monkey and human neocortex. J Comp Neurol 303:584–599
21. Hirano A, Zimmermann HM (1962) Alzheimer's neurofibrillary changes: a topographical study. Arch Neurol 7:227–242
22. Hsiao K, Chapman P, Nilsen S, Eckman C, Harigaya Y, Younkin S, Yang F, Cole G (1996) Correlative memory deficits, Aβ elevation and amyloid plaques in transgenic mice. Science 274:99–102
23. Ishii T (1966) Distribution of Alzheimer's neurofibrillary changes in the brain stem and hypothalamus of senile dementia. Acta Neuropathol 6:181–187
24. Katsuno T, Morishima-Kawashima M, Saito Y, Yamanouchi H, Ishiura S, Murayama S, Ihara Y (2005) Independent accumulations of tau and amyloid β-protein in the human entorhinal cortex. Neurologist 64:687–692
25. Kitamoto T, Ogomori K, Tateishi J, Prusiner SB (1987) Formic acid pretreatment enhances immunostaining of cerebral and systemic amyloids. Lab Invest 57:230–236
26. Koutcherov Y, Mai JK, Ashwell KWS, Paxinos G (2002) Organisation of human hypothalamus in fetal development. J Comp Neurol 423:299–318
27. Kremer HPH, Roos RAC, Dingjan G, Marani E, Bots GThAM (1990) Atrophy of the hypothalamic lateral tuberal nucleus in Huntington's disease. J Neuropathol Exp Neurol 49:371–382
28. Kremer HPH, Swaab DF, Bots GThAM, Fisser B, Ravid R, Roos RAC (1991) The hypothalamic lateral tuberal nucleus in Alzheimer's disease. Ann Neurol 29:279–284
29. Kremer HPH (1992) The hypothalamic lateral tuberal nucleus: normal anatomy and changes in neurological diseases. Prog Brain Res 93:249–261
30. Lazarov O, Robinson J, Tang Y-P, Hairston IS, Korade-Mirnics Z, Lee VM-Y, Hersh LB, Sapolsky RB, Mirnics K, Sisodia SS (2005) Environmental enrichment reduces Aβ levels and amyloid deposition in transgenic mice. Cell 120:701–713
31. Lee H-G, Casadesus G, Zhu X, Joseph JA, Perry G, Smith MA (2004) Perspectives on the amyloid-β cascade hypothesis. J Alzheimers Dis 6:137–145
32. Lee H-G, Perry G, Moreira PI, Garrett MR, Liu Q, Zhu X, Takeda A, Nunomora A, Smith MA (2005) Tau phosphorylation in Alzheimer's disease: pathogen or protector? Trends Mol Med 11:164–169

33. Leissring MA, Farris W, Chang AY, Walsh DM, Wu X, Sun X, Frosch MP, Selkoe DJ (2003) Enhanced proteolysis of β-amyloid in APP transgenic mice prevents plaque formation, secondary pathology, and premature death. Neuron 40:1087–1093
34. Lenders M-B, Peers M-C, Tramu G, Delacourte A, Defossez A, Petit H, Mazzuca M (1989) Dystrophic peptidergic neurites in senile plaques of Alzheimer's disease hippocampus precede formation of paired helical filaments. Brain Res 481:344–349
35. Lewis J, Dickson DW, Lin W-L, Chisholm L, Corral A, Jones G, Yenn S-H, Sahara N, Skipper L, Yager D, Eckman C, Hardy J, Hutton M, McGowan E (2001) Enhanced neurofibrillary degeneration in transgenic mice expressing mutant tau and APP. Science 293:1487–1491
36. Liu R-Y, Zhou J-N, Hoogedijk WJG, van Heerikhuize J, Kamphorst W, Ummehopa UA, Hofman MA, Swaab DF (2000) Decreased vasopressin gene expression in the biological clock of Alzheimer disease patients with and without depression. J Neuropathol Exp Neurol 59:314–332
37. Mengod G, Rigo M, Savasta M, Probst A, Palacios JM (1992) Regional distribution of neuropeptide somatostatin gene expression in the human brain, Synapse 12:62–74
38. Mercken M, Vandermeeren M, Lubke U, Six J, Boons J, Van de Voorde A, Martin J-J, Gheuens J (1992) Monoclonal antibodies with selective specificity for Alzheimer tau are directed against phosphatase-sensitive epitopes. Acta Neuropathol 84:265–272
39. Morrison JH, Benoit R, Magistretti PJ, Bloom FE (1983) Immunohistochemical distribution of pro-somatostatin-related peptides in cerebral cortex. Brain Res 262:344–351
40. Mufson EJ, Benoit R, Mesulam MM (1988) Immunohistochemical evidence for a possible somatostatin-containing amygdalostriatal pathway in normal and Alzheimer's disease brain. Brain Res 453:117–128
41. Najimi M, Chigr F, Leduque P, Jordan D, Charnay Y, Chayville JA, Tohyama M, Kopp N (1989) Immunohistochemical distribution of somatostatin in the infant hypothalamus. Brain Res 483:205–220
42. Najimi M, Jordan D, Chigr F, Champier J, Kopp N, Slama A, Bertherat J, Videau C, Epelbaum J (1991) Regional distribution of somatostatin binding sites in the human hypothalamus: a quantitative autoradiographic study. Neuroscience 40:321–335
43. Oddo S, Caccamo A, Shepherd JD, Murphy MP, Golde TE, Kayed R, Metherate R, Mattson MP, Akbari Y, LaFerla FM (2003) Triple-transgenic model of Alzheimer's disease with plaque and tangles: intracellular Aβ deposits and synaptic dysfunction. Neuron 39:409–421
44. Oddo S, Caccamo A, Kitazawa M, Tseng BP, LaFerla FM (2003) Amyloid deposition precedes tangle formation in a triple transgenic mice model of Alzheimer's disease. Neurobiol Aging 24:1063–1070
45. Reubi JC, Cortes R, Maurer R, Probst A, Palacios JM (1986) Distribution of somatostatin receptors in the human brain; an autoradiographic study. Neuroscience 18:329–346
46. Romijn HJ, Van Uum JF, Emmering J, Goncharuk V, Buijs RM (1999) Colocalization of VIP with AVP in neurons of the human paraventricular, supraoptic and suprachiasmatic nucleus. Brain Res 832:47–53
47. Rudelli RD, Ambler MW, Wisniewski HM (1984) Morphology and distribution of Alzheimer neuritic (senile) and amyloid plaques in striatum and diencephalon. Acta Neuropathol 64:273–281
48. Salehi A, Van de Nes JAP, Hofman MA, Gonatas NK, Swaab DF (1995) Early cytoskeletal changes as shown by Alz-50 are not accompanied by decreased neuronal activity. Brain Res 578:29–39
49. Saper CB, German DC (1987) Hypothalamic pathology in Alzheimer's disease. Neurosci Lett 74:364–370
50. Saper CB (1990) Hypothalamus. In: Paxinos G (ed) The human nervous system. Academic, San Diego, CA, pp 389–413
51. Schultz C, Koppers D, Sassin I, Braak E, Braak H (1998) Cytoskeletal alterations in the human tuberal hypothalamus related to argyrophilic grain disease. Acta Neuropathol 96:596–602
52. Schultz C, Ghebremedhin E, Braak E, Braak H (1999) Sex-dependent cytoskeletal changes of the human hypothalamus develop independently of Alzheimer's disease. Exp Neurol 160:186–193
53. Standaert DG, Lee VM-Y, Greenberg BD, Lowery DE, Trojanowski JQ (1991) Molecular features of hypothalamic plaques in Alzheimer's disease. Am J Pathol 139:681–691
54. Stopa EG, Volicer L, Kuo-Leblanc V, Harper D, Lathi D, Tate B, Satlin A (1999) Pathologic evaluation of the human suprachiasmatic nucleus in severe dementia. J Neuropathol Exp Neurol 58:29–39
55. Swaab DF (2003) Lateral tuberal nucleus. In: Aminoff MJ, Boller F, Swaab DF (eds) Handbook of clinical Neurology, vol 79, The human hypothalamus: basic and clinical aspects, Part 1: Nuclei of the hypothalamus. Elsevier, Amsterdam, pp 263–268
56. Timmers HJLM, Swaab DF, Van de Nes JAP, Kremer HPH (1996) Somatostatin$_{1-12}$ immunoreactivity is decreased in the hypothalamic lateral tuberal nucleus of Huntington's disease patients. Brain Res 728:141–148
57. Van de Nes JAP, Kamphorst W, Ravid R, Swaab DF (1993) The distribution of Alz-50 immunoreactivity in the hypothalamus and adjoining areas of Alzheimer's disease patients. Brain 116:103–115
58. Van de Nes JAP, Sluiter AA, Pool CW, Kamphorst W, Ravid R, Swaab DF (1994) The monoclonal antibody Alz-50, used to reveal cytoskeletal changes in Alzheimer's disease, also reacts with a large subpopulation of somatostatin neurons in the human hypothalamus and adjoining areas. Brain Res 655:97–109
59. Van de Nes JAP, Kamphorst W, Ravid R, Swaab DF (1998) Comparison of β-protein/A4 deposits and Alz-50-stained cytoskeletal changes in the hypothalamus and adjoining areas of Alzheimer's disease patients: amorphic plaques and cytoskeletal changes occur independently. Acta Neuropathol 96:129–138
60. Van de Nes JAP, Sandmann-Keil D, Braak H (2002) Interstitial cells in the entorhinal region expressing somatostatin-28 immunoreactivity are susceptible to develop Alzheimer's disease-related cytoskeletal changes. Acta Neuropathol 104: 351–356